18TH WORLD CONFERENCE ON EARTHQUAKE ENGINEERING
WCEE2024
MILAN

MILAN, ITALY
30TH JUNE - 5TH JULY 2024
www.wcee2024.it

USING MARKOV CHAINS TO INVESTIGATE THE SENSITIVITY OF FRICTION ISOLATORS TO GROUND MOTION DURATION

D. Ruggiero[1] & G.M. Calvi[2]

[1] EPFL (École Polytechnique Fédérale de Lausanne), Lausanne, Switzerland, david.ruggiero@epfl.ch

[2] Scuola Universitaria Superiore IUSS, Pavia, Italy

Abstract: *Base isolation using friction devices offers an appealing structural solution for mitigating seismic risk. However, the plastic behaviour of friction isolators can lead to large residual displacements, particularly in long duration earthquakes. In order to meet serviceability requirements, it is necessary to be able to predict and limit these displacements. In this paper, it is shown how the seismic input to a friction isolator may be treated as a series of independent impulses, allowing the total response to be formulated as a stochastic process. Under this framework, the movement of the isolator resembles Brownian motion and classical results can be leveraged to predict the evolution of the probability distribution for position of the slider as a function of ground motion duration. In order to extend the analysis to friction devices with arbitrary backbone curves, a novel numerical method using Markov chains is introduced and applied to four different types of friction sliders. Validation of the proposed model is performed by comparing the Markov chain method to nonlinear time history analysis using a large suite of artificial earthquake records, generated to explicitly control for earthquake duration and power spectrum. The validation confirms the accuracy of the Markov chain analysis and provides valuable insights into the duration-dependency of residual displacements in different types of friction isolation systems.*

1 Introduction

In the field of earthquake engineering, base isolation has emerged as one of the most effective strategies for ensuring a high level of structural performance under seismic loading. The benefits of base isolation are twofold: firstly, by increasing the effective period of vibration the structural response is shifted into a more favourable regime, and secondly, by adding a hysteretic damping component overall forces and displacements are lowered.

One of the simplest types of structural isolator is a flat friction slider (also known as a Coulomb slider), whose hysteresis can be idealized as a rectangular loop with infinite loading and unloading stiffness and a constant frictional force. Such a device has no re-centring capacity and can thus develop large residual displacements after a seismic event. This problem can be mitigated by coupling it in parallel with an elastic element or by employing curved sliders (also known as friction pendulum systems), which have the benefit that gravity provides a re-centring tendency and have found widespread use. Other types of variable friction devices have also been proposed and validated (Calvi & Ruggiero, 2015; Calvi, Moratti, & Calvi, 2016; Calvi, Yang, & Wiebe, 2020; Shang, Tan, Zhang, Han, & Qin, 2021; Tan, Shang, Han, Yang, & Zhang, 2023).

The behavioural similarity of all friction devices is that they are predominantly plastic mechanisms; that is, when the load is removed, a plastic offset displacement remains. As a result, they form very broad hysteresis

loops that do not pass through the origin. This is in contrast to elastic elements with viscous damping that will return to rest near to their initial location after excitation.

When designing a friction base isolation system, the range of movement of the device is an important response parameter for serviceability considerations (e.g., isolator dimensions, mechanical linkages, recentring the structure after an earthquake). In particular, it is important to be able to estimate the magnitude of residual displacements after the earthquake, as this dictates the viability of continued use of the structure.

Most modern seismic design methods (both force- and displacement-based) idealize structural response using an equivalent linear elastic system, and thus do not provide a means for estimating residual displacements of plastic mechanisms. Whereas a linear elastic system will always return to the origin regardless of the duration of the ground motion, a friction system can tend to “migrate” over an increasingly large distance the longer the excitation lasts. Simple methods for evaluating this dependency, however, have not yet been developed, and solution by nonlinear time history analysis (NLTHA), while accurate, remains computationally intensive and requires assembling a suite of suitable ground motions as input.

One behaviour in particular of plastic mechanisms is incompatible with the equivalent linear approximation; namely, the accumulation of plastic offsets as time passes. In this way the displacements of a friction slider can be equated to that of a random walk or Brownian motion. It is well known that the expected displacement for a Brownian system increases monotonically as a function of time (Einstein, 1906), and one may imagine that a frictional isolator would have similar characteristics.

By analogy with the random walk, the duration of ground motion should be an important, and potentially negative, factor in the design and analysis of friction devices. Though the duration of earthquake events can vary widely (Hancock & Bommer, 2007; Trifunac & Brady, 1975), this variability is not accounted for explicitly in current design codes except for in a cursory fashion with special rules for near-field ground motions. There is an implicit consideration of the duration effect through the use of response spectra, since longer seismic events generated using the same parameters will tend to have higher spectral ordinates. However, the relationship between duration and displacements is obfuscated by the introduction of spectra; two events with similar spectra but different durations will cause different behaviour of frictional systems.

This paper develops a method for predicting the duration-dependency of residual displacements for idealized friction-type isolators. In particular, it will seek to compare the behaviour of four different devices with distinct hysteresis shapes as shown in Figure 1: the Flat Slider, Friction Pendulum, BowTie, and BowC. In doing so, the dependency on the length of the ground motion will be explicitly considered, in recognition of the aforementioned duration effect.

In the first part of this work, a novel stochastic procedure using Markov chains is proposed for the analysis of rigid-plastic systems like friction devices. In the second half of this study, a series of numerical NLTHAs using artificial ground motions of different durations is conducted. These results are used to validate the Markov chain method and show that it captures the dependency of residual displacements of friction systems on earthquake duration.

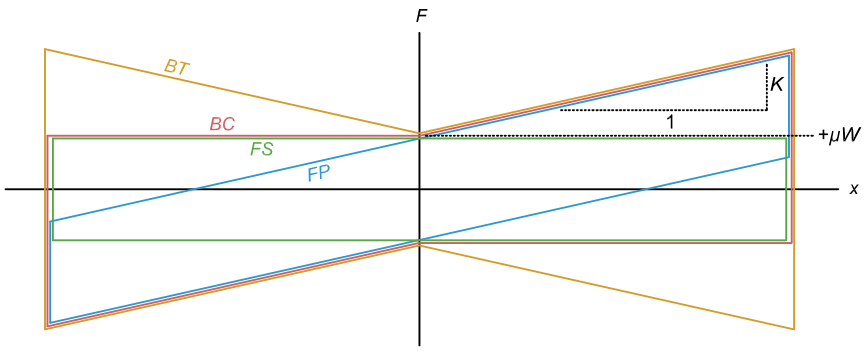

Figure 1. Force-displacement backbone shapes for four types of friction devices (FS = Flat Slider, FP = Friction Pendulum, BT = BowTie, BC = BowC).

2 Stochastic model

Considering the stepwise movements of a friction slider to be akin to a random walk, it is appropriate to investigate the behaviour using a probabilistic analysis. While stochastic methods have been previously applied to the problem of hysteretic behaviour, some of these analyses have either considered only flat sliders (Crandall, Lee, & Williams, 1974; Caughey & Dienes, 1961) or have focussed on general elastoplastic mechanisms and have been limited to more theoretical discussion (Paparizos & Iwan, 1988). Building on these works, it will be possible to develop more practical stochastic methods to predict the residual and maximum displacements of generic friction devices.

As a starting point for a general method, the mechanics of the simplest friction device (the flat slider) will first be considered. This device is characterized by an infinite (or nearly infinite) loading/unloading stiffness and a flat “yield” plateau. The behaviour is symmetric; that is, the response at any point is indistinguishable from that at any other (within the displacement limits of the device). This property in particular makes the flat slider ideal for closed-form stochastic analysis. In reality, frictional resistance is also a function of other parameters such as velocity, pressure and temperature (Papageorgiou & Constantinou, 1990); the derivation that follows is for an idealized device, however, a more detailed consideration of these effects could also be included in later refinements to this model.

The fact that the tangent stiffness of the flat slider is always either infinite or zero simplifies the equations of motion and as a result it does not experience resonance in the same way as an elastic element. Assuming a single degree-of-freedom (SDOF) model as shown in Figure 2, the maximum net force that the mass can experience (and thus the maximum acceleration) is equal to the force of friction. There is no amplification on account of resonance, which makes closed-form analysis straightforward.

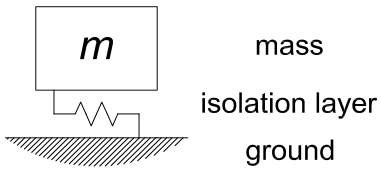

Figure 2. Idealized single degree-of-freedom isolator model.

When examining relative acceleration between the ground and the superstructure, a friction slider acts as a filter; only ground accelerations that are larger than the friction coefficient multiplied by the gravitational constant induce the structure to move. Figure 3 illustrates this effect for different friction coefficient ratios. For moderate values of friction, the behaviour from the point of view of the supported mass resembles a series of independent acceleration spikes or pulses. The sparseness of these pulses depends on the ratio between the friction coefficient and the amplitude of the ground acceleration, defined here as α:

$$\alpha = \frac{\sigma}{\mu g} \tag{1}$$

where σ represents the standard deviation of the ground accelerations, μ is the initial friction coefficient of the system, and g is the acceleration of gravity.

The quantity α represents the relative degree of isolation. As α grows larger the isolation effect becomes more significant; conversely, for a small α, the sliding friction activates only for the strongest pulses in the ground motion.

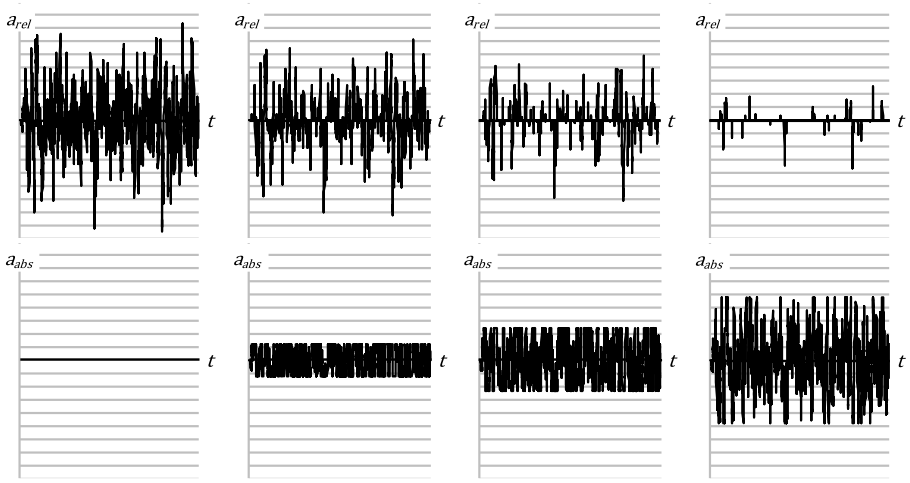

Figure 3. Acceleration of isolated mass relative to the ground (top) and absolute acceleration of mass (bottom) as a function of degree of isolation for a flat slider.

The acceleration pulses will result in a stepwise displacement of the mass, as shown in Figure 4. When the friction coefficient is low enough, the pulses are independent; that is, the mass experiences relative movement from each pulse independently. The total motion at any point in time is the sum of all of the preceding displacement steps. Determining a statistical model for the size of the steps will therefore lead to a statistical model for the displacement at any point in time, from which maximum and residual displacements may be calculated as a function of duration.

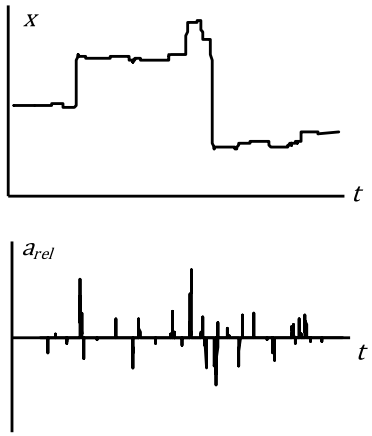

Figure 4. Stepwise movement of a flat friction isolator caused by pulses in the filtered ground motion: a displacement (x, top) is induced only by cycles with a peak acceleration (a_{rel}, bottom) larger than μg.

In the case of a flat slider, symmetry ensures that the probabilistic distribution for displacement step size is independent of the location of the slider; however, this is not the case in general for other isolator typologies. If the size of the i-th step is notated as the random variable D_i, then the total displacement after n steps is given by:

$$X_n = D_1 + \cdots + D_n = \sum_i D_i \tag{2}$$

X_n is itself a random variable, the distribution of which depends on the underlying distribution for D. Given a distribution for D, therefore, one may calculate the distribution for X_n through a convolution integral. However, in general as n grows large, the Central Limit Theorem (CLT) of statistics states that the sum of a number of independent random variables will be approximately normally distributed, independent of the underlying distributions of the summands (Billingsley, 1995). Furthermore, for any n the variance of the sum is equal to the sum of the variances:

$$\sigma_{X_n}^2 = \sum_i \sigma_{D_i}^2 \tag{3}$$

For the particular case of a flat slider, each displacement increment is an identical and independent random variable (due to symmetry), therefore:

$$\sigma_{X_n}^2 = n \cdot \sigma_D^2 \tag{4}$$

$$\sigma_{X_n} = \sqrt{n} \cdot \sigma_D \tag{5}$$

In summary, the total displacement of the flat slider after n impulses converges to a normally distributed random variable with standard deviation proportional to the square root of n:

$$X_n \sim N(0, n \cdot \sigma_D^2) \tag{6}$$

By extension, the absolute value of displacement will exhibit a half-normal distribution, the mean of which is given by the classical result:

$$\mu_{|X_n|} = \sigma_{X_n} \cdot \sqrt{\frac{2}{\pi}} = \sigma_D \cdot \sqrt{\frac{2n}{\pi}} \tag{7}$$

Therefore, the dispersion and the expected value of the displacement increase as the number of acceleration pulses increases; that is, as the duration of the seismic event increases. This result confirms the intuitive understanding of the behaviour. Since residual displacement for a friction slider is simply equal to the displacement at the end of the seismic event, its distribution is the same as that given above.

It should be noted that this simple model for the movement of a friction slider is indeed mathematically equivalent to a random walk. More specifically, it represents a Wiener process, used to model Brownian motion among other phenomena. Therefore, statistical results from these well-established areas of research may be immediately applied to the case of the flat slider as well (e.g., maximum displacements as a function of time). In this paper, however, only the application to residual displacements is considered.

While the analytical formulation above gives a satisfying explanation for the movements of the flat slider, it is limited in scope because of the assumption that the behaviour is symmetric at every point. In order to model more complex plastic phenomena (i.e., arbitrary hysteresis shapes), it is necessary to generalize the procedure to allow for the possibility that the step sizes, D_i, are not identically distributed. For this general case a closed form analytical solution such as the preceding becomes unwieldy and therefore it is more practical to develop a numerical solution procedure for the probability distributions discussed above.

3 Numerical evaluation using Markov chains

The above derivation has used stochastic analysis to illustrate the duration dependency for the behaviour of a flat slider, a rigid-plastic mechanism where the response at any point is identical. In order for this to be a practical analysis technique, the method can be extended to consider cases where the behaviour is not the same at every location; e.g., friction pendulum and variable friction systems. To this end, it is necessary to develop a method for calculating the underlying probability distribution for D; that is, the displacement step size.

The size of the displacement step will depend on the magnitude of the acceleration pulse that the isolator experiences as well as the current position of the slider. The acceleration pulse magnitude can itself be represented as a random variable with a distribution that depends on the ground motion. If the power spectrum of the ground motion is known, then the ground accelerations follow a normal distribution with variance σ^2 equal to the integral of the power spectrum (Mohraz & Sadek, 2001). This will serve as the input to the general stochastic model; given the distribution of the random variable A representing the magnitude of the acceleration pulses, the distribution of step sizes D at any starting location X can be calculated.

It may be noted that the distribution for D need not be symmetric. For example, considering the BowC hysteresis at large positive displacements, a pulse in the positive direction causes less movement than a pulse in the negative direction because of the unequal forces for the positive and negative branches of the hysteretic loop.

For all but the simplest cases it will be impossible to find a closed form solution for the probability distribution of the resting position after a pulse. Therefore, a numerical approach using Markov processes (Norris, 1998) will be pursued instead.

A Markov process is characterized by a transition matrix defining the probability of arriving in a certain state S_j from another state S_i. For a SDOF system the states are the possible positions; it is necessary to discretize the values into bins over a finite domain, although with a fine enough discretization the results will approximate the continuous solution. The Markov transition matrix therefore gives the probability that the isolator will displace from any point to any other point when subjected to a single pulse. Knowing this, standard Markov chain operations can be used to calculate the probability distributions for maximum and residual displacement.

The Markov transition matrix is generated in practice by calculating the distribution for D at every point X on the range of motion of the friction device. This will be done here using mechanical considerations to calculate the stopping distance (i.e., distance of travel) of the mass atop the isolator when it is subjected to an acceleration pulse.

The area of each relative acceleration spike (Figure 5) experienced by the mass represents an impulse J applied to the system. The magnitude of this impulse may be calculated by assuming a characteristic shape for these pulses. In this work the pulses have been taken as Ricker wavelets, which have an established history of use in seismology (Ricker, 1953). In general, the impulse experienced will depend on the starting position X, which will dictate the effective frictional force for movement in the positive and negative directions. Notating the positive backbone as F_f^+ and the negative backbone as F_f^-, the impulse caused by a certain acceleration pulse intensity A at position X is calculated as:

$$J(A,X) = -\iint_R dF \cdot dt \tag{8}$$

where:

the region R = represents the area outside of $F_f^-(x)$ and $F_f^+(x)$ bounded by $F(t)$,

the force $F(t) = m \cdot a \cdot w(t)$

$w(t)$ is the wavelet shape as a function of time t.

This integral is represented by the shaded area in the left pane of Figure 5.

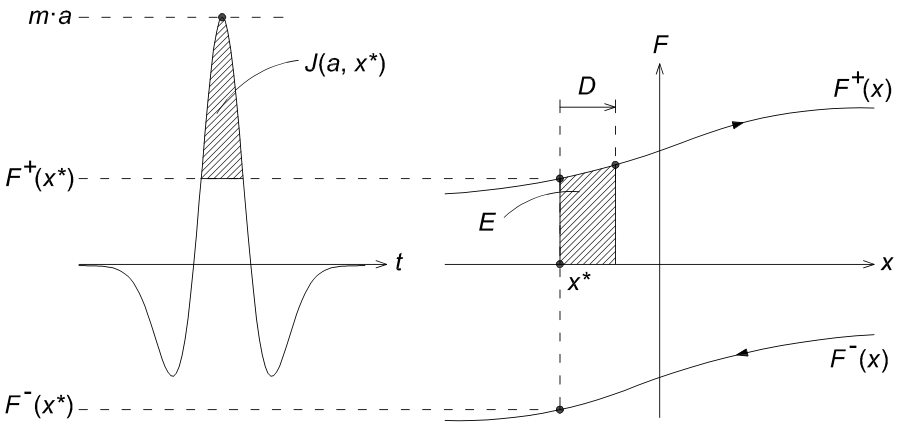

Figure 5. Calculation of impulse (left) and stopping distance (right) for a given acceleration pulse.

If it is assumed that the pulses are disperse enough to allow the mass to come to rest in between inputs, then the velocity after an impulse of J is:

$$V = \frac{J}{m} \tag{9}$$

The kinetic energy of the mass following a pulse is therefore:

$$E(J) = \frac{1}{2} \cdot mV^2 = \frac{J^2}{2m} \tag{10}$$

The mass will come to rest after this energy has been dissipated by the frictional mechanism. This amounts to an integration of the area under the force-displacement diagram for the slider:

$$E(A,X) = \frac{J(A,X)^2}{2m} = \begin{cases} \int_X^{X+D} F_f^+(t) \cdot dt & \text{if} \quad J \geq 0 \\ \int_X^{X+D} F_f^-(t) \cdot dt & \text{if} \quad J < 0 \end{cases} \tag{11}$$

This integral equation is then solved to find the stopping distance D as a function of A and X. The inversion of the integral must be calculated numerically with iteration, except for in the simplest cases (e.g., flat slider). This procedure is shown graphically in the right pane of Figure 5.

Finally, a new position Y may be calculated as the sum of the starting position and the displacement:

$$Y = X + D \tag{12}$$

As a caveat, if the calculated stopping distance would bring the system into a location where $F_f^-(Y) > 0$ or $F_f^+(Y) < 0$ then the stopping distance should be revised to arrive at the intercept directly. This is to account for the fact that the system cannot be in static equilibrium with an unbalanced force on it and will subsequently find the nearest equilibrium state. As an immediate result, it can be seen that there will be zero probability of coming to rest in one of these unstable zones. This is particularly relevant for friction pendulum systems, which in some regards fall on the boundary of usability of this method.

At this point it is necessary to recall that each intermediate term in the calculation is a random variable. Given a probability distribution for ground accelerations, $f_A(a)$, it is then possible to calculate the conditional probability distribution for the new position given the starting position; that is, $f_{Y|X}(y|x)$. This is precisely the Markov transition matrix. For numerical evaluation, the distribution for A should be discretized into bins along with the spatial dimension.

In order to generate the transition matrix, it is necessary to calculate the ending position (state S_y) for every possible starting position (state S_x) and every possible acceleration pulse (A) over the discretized domain. The matrix (originally initialized to zeroes) is generated by iterating over S_x and A, calculating J and consequently Y from these inputs, and adding the probability $P(A)$ to the matrix entry corresponding to S_y.

Sample transition matrices for the four friction devices are visualized in Figure 6, with the colour scale representing probability and the x and y axes representing starting position and ending position, respectively. A total of 201 bins have been used in the spatial discretization. Certain aspects of the behaviour of the device can be ascertained directly from the transition matrix. The high probability along the diagonal indicates that for every possible position, the most likely occurrence is for the isolator to remain still; this is the effect of all pulses smaller than the friction force. For the friction pendulum and BowC devices the asymmetric hysteresis is also apparent: when the starting displacement is positive, the slider is more likely to move to the left; when it is negative, it is more likely to move to the right.

Having generated the transition matrix, the probability of being in a certain state after n cycles is calculated simply by repeated matrix multiplication:

$$\langle \mathbf{P_n} \rangle = \langle \mathbf{P_{n-1}} \rangle [\mathbf{T}] \tag{13}$$

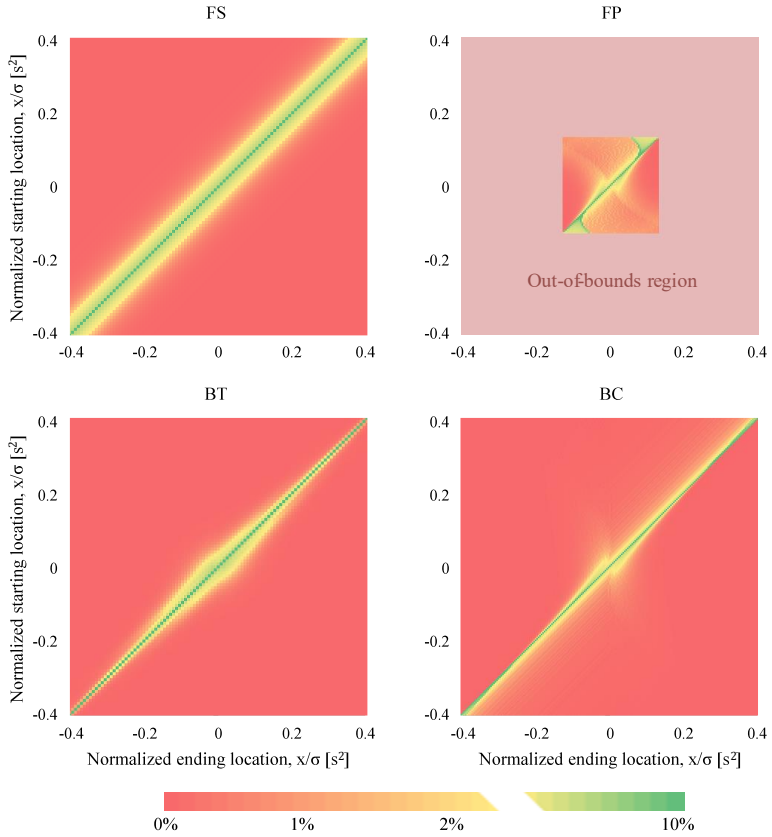

Figure 6. Markov transition matrix for each device, probabilities visualized using the colour scale.

In the initial state there is 100% probability of being at the zero position (which can have an arbitrary index, but is taken here as the first state):

$$\langle \mathbf{P_0} \rangle = \langle 1 \quad 0 \quad \cdots \quad 0 \rangle \tag{14}$$

Therefore:

$$\langle \mathbf{P_n} \rangle = \langle \mathbf{P_0} \rangle [\mathbf{T}]^n \tag{15}$$

Repeated multiplications of the transition matrix results in the evolution of the probability distribution as a function of the number of impulses applied. Knowing the PDF for position as a function of time one may directly predict the average residual displacements as a function of earthquake duration by taking the mean of the distribution. Other parameters such as variability of the residual displacement can also be directly calculated.

4 Validation via Nonlinear Time History Analysis

In order to validate the Markov chain procedure for comparing residual displacements for different shaking durations, a series of nonlinear time history analyses was conducted. Each NLTHA subjects a SDOF system comprising of a mass atop a friction device to a ground acceleration. For simplicity, only uniaxial behaviour has been considered.

For sake of direct comparison, the same initial friction coefficients and secondary stiffnesses have been used for all four devices, thus the backbone curves resemble those shown in Figure 1. Velocity, temperature, and pressure effects have been ignored and it is assumed that the frictional behaviour is perfectly rigid.

In order to obtain detailed information about the statistical distributions of the response parameters of interest, a large suite of ground motions is required as input. While scaled real-world accelerograms provide more realistic record-by-record response, using ground motions from different sources and conditions would introduce additional sources of uncertainty into the analysis and greatly limit the potential number of analyses that could be run. Therefore, the NLTHAs were instead conducted using artificial accelerograms. Though not necessarily realistic in the time domain, using artificial accelerograms allowed for more control of extraneous variables; all of the ground motions in each suite were constructed to have identical frequency content, power

spectrum, duration, and envelope shapes. This provides a useful, systematic method for comparing the behaviour of different types of hystereses as an explicit function of duration.

The artificial accelerograms were generated based on the method of Gasparini and Vanmarcke (1977) as a superposition of sinusoids with random phase according to specified weightings. The weightings are calculated via the power spectral density function, in this case following the model by Tajimi (1960) with the suggested values of $\omega_g = 4\pi$ and $\xi_g = 0.60$. Baseline correction was performed using a fourth-order high-pass Bessel filter as suggested by Boore and Bommer (2005). It should be noted that the records were not matched to any particular response spectrum. Instead, they were all generated using the same power spectrum in order to simulate different events caused by the same source. As a result, the peak ground acceleration and other spectral quantities vary among the artificial records.

Since the summation of sinusoids produces a stationary process of undefined length, it is necessary to apply an envelope function to produce the overall "shape" of the peaks of the accelerogram. In order to allow comparison with the theoretical predictions, a square envelope has been used as the base case, since it provides a distribution of acceleration intensities that does not vary with time.

NLTHA was conducted using a SDOF Newmark solver (Newmark & Rosenblueth, 1971) with parameters $\gamma = 0.5$, $\beta = 0.25$, a time step of 0.001s, and a force-convergence threshold of 10^{-5} N. The results have been non-dimensionalized by dividing by the standard deviation of the ground accelerations, σ. The displacements will scale by this intensity measure provided that α (the relative degree of isolation, defined in Equation 1) and ω are held constant, where:

$$\omega^2 = \frac{k}{m} \tag{16}$$

with k equal the stiffness of the system following motion inception and m equal to the mass of the isolated structure. The quantity ω is analogous to the circular frequency in a linear elastic system, calculated here using the secondary stiffness k. As displacements become very large, this is the limiting natural frequency of the device.

For the present study α has been taken as 2.5, representing a relatively high level of isolation; ω^2 has been taken as 3.0, corresponding to a natural period of vibration of 3.63 seconds. This represents the period of vibration for the isolator considering the superstructure as a rigid mass, which is in the range of typical values for industrially available friction pendulum systems (Sarkisian, Lee, Long, Shook, & Díaz, 2013).

The primary variable in the present study was the duration of the ground motion. 150 independent ground motions were generated for each duration between 10 seconds and 90 seconds at an interval of 10 seconds. This same suite of ground motions was then used in combination with different isolator hystereses to produce a tree of analysis cases. For each analysis the statistic of residual displacement was extracted; from the entire suite of analyses an estimate can be made of the probabilistic distribution of residual displacement as a function of ground motion duration.

Note that since the treatment of time in the Markov model is discretized, therefore for comparison with the NLTHA results it is necessary to define a scale factor to account for the "pulse rate". In this research the value of this scale factor has been selected as 0.75 seconds per pulse. This is close to the frequency ω_g used to generate the artificial time histories, and provides good correlation with the NLTHA analyses. However, future studies should clarify the derivation and role of this factor in the analysis.

Figure 7 shows the comparisons of the residual displacement estimates between the Markov method and the NLTHA averages for each of the four friction devices considered. Furthermore, one may also compare the shape of the predicted probability distributions to the cumulative probability densities of the nonlinear analyses; this is shown for 10 seconds and 90 seconds in Figure 8.

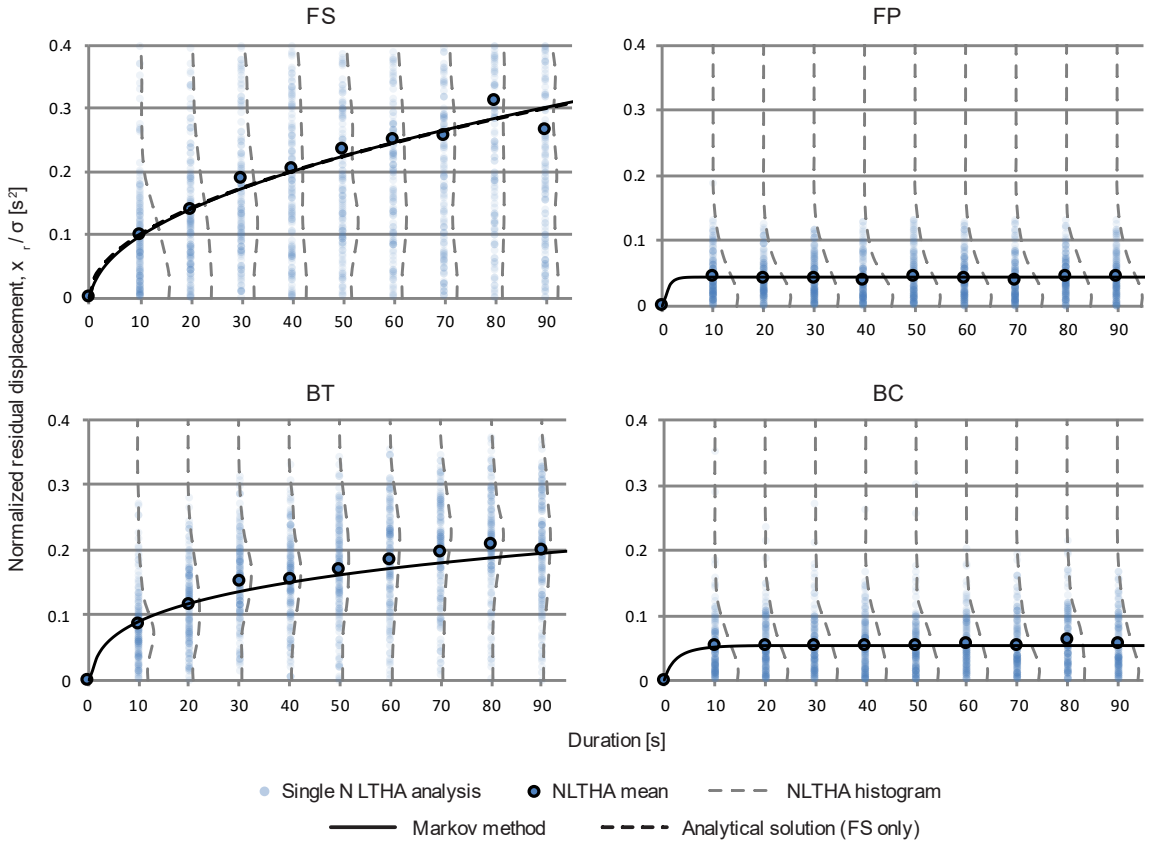

Figure 7. Comparison between Markov chain analysis and NLTHA results for residual displacement.

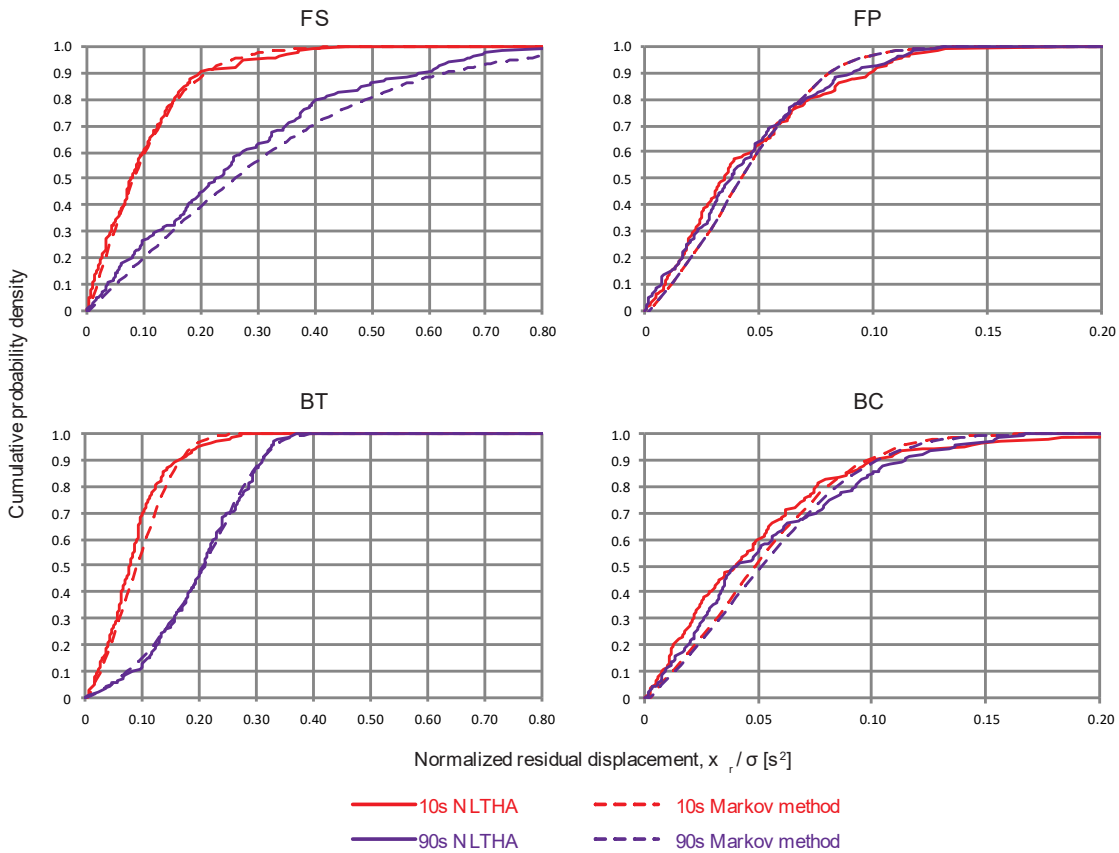

Figure 8. Comparison between Markov chain analysis and NLTHA cumulative probability densities for residual displacement (10s and 90s duration).

The agreement of the expected and average values of residual displacement is in each case quite good. The increasing trend for the BowTie and flat slider, and the plateau for the friction pendulum and BowC devices are captured very accurately. The Markov chain results for the flat slider are virtually indistinguishable from the form of the analytical square-root solution (also shown in Figure 7, although the lines are essentially coincident). Small errors in these predictions could be dependent on the details of the intermediate steps of the analysis (e.g., what shape of wavelet is used for ground acceleration pulses).

The evolution of the shape of the probabilistic distribution is also captured well, as illustrated by the cumulative distribution functions (CDFs) shown in Figure 15. For the BowTie and flat slider, an increase in dispersion is predicted as the duration is increased, as also seen in the NLTHA analysis results. The friction pendulum and the BowC on the other hand have probability distributions that remain stationary; the CDFs for all durations essentially overlap.

In general, these results suggest that the Markov chain method is an accurate means for determining the probability distribution of residual displacements for friction sliders as a function of duration. Application of this approach provides useful insight about the behaviour of different types of sliders under increasing ground motion duration, and could be a useful tool in developing design rules for such systems.

5 Conclusions

This paper has presented a method for predicting the influence of ground motion duration on the behaviour of friction isolators. In particular, it has developed a novel stochastic procedure using Markov chains to calculate a probability distribution for slider position as a function of time, allowing direct evaluation of the expected residual displacement of the device at the end of the ground motion.

The stochastic procedure was validated by comparison to the results of a numerical study in which four different types of hysteretic shape representing different friction isolator designs were subjected to over one thousand artificially generated ground motions via explicit nonlinear time history analysis. The trends for both mean values and probability distributions of residual displacements match closely, although future research is still needed to investigate the pulse rate used for the Markov analyses and to extend the results to more realistic ground motion inputs in lieu of artificial records. Nonetheless, at a minimum this method provides a means for comparing relative behaviour of different types of isolators under controlled conditions, and for describing the shape of the dependency of residual displacement on duration.

By providing a mechanically-based means of estimating the time-dependent probability distribution of displacements in friction devices, the present research opens the door to more accurate analysis and design of isolation systems. It allows for calculation of objective metrics for the comparison of different frictional devices, such as their re-centring tendency and sensitivity to duration effects, as well as a quantitative model for estimating residual displacement.

6 References

Billingsley, P. (1995). *Probability and Measure* (Third ed. ed.). New York: John Wiley & Sons.

Boore, D. M., & Bommer, J. J. (2005). Processing of strong-motion accelerograms: needs, options and consequences. *Soil Dynamics and Earthquake Engineering, 25*(2), 93-115.

Calvi, P. M., & Ruggiero, D. M. (2015). Numerical Modeling of Variable Friction Sliding Base Isolators. *Bulletin of Earthquake Engineering, 14*(2), 549-568.

Calvi, P. M., Moratti, M., & Calvi, G. (2016). Seismic isolation devices based on sliding between surfaces with variable friction coefficient. *Earthquake Spectra, 32*(4), 2291-2315.

Calvi, P. M., Yang, T. -Y., & Wiebe, R. (2020). Development of variable friction pendulum systems. Sendai, Japan: Proceedings of the 17th World Conference on Earthquake Engineering.

Caughey, T. K., & Dienes, J. K. (1961). Analysis of a Nonlinear First-Order System with a White Noise Input. *Journal of Applied Physics, 32*(11), 2476-2479.

Crandall, S. H., Lee, S. S., & Williams, J. H. (1974). Accumulated Slip of a Friction-Controlled Mass Excited by Earthquake Motions. *ASME Journal of Applied Mechanics, 41*(4), 1094-1098.

Einstein, A. (1906). Zur Theorie der Brownschen Bewegung. *Annalen der Physik, 324*(2), 371-381.

Gasparini, D. A., & Vanmarcke, E. H. (1977). *Simulated earthquake motions compatible with prescribed response spectra.* Cambridge, USA: Department of Civil Engineering Research Report R76-4.

Hancock, J., & Bommer, J. J. (2007). Using spectral matched records to explore the influence of strong-motion duration on inelastic structural response. *Soil Dynamics and Earthquake Engineering, 27*(4), 291-299.

Mohraz, B., & Sadek, F. (2001). Earthquake Ground Motion and Response Spectra. In F. Naeim (Ed.), *The Seismic Design Handbook* (pp. 47-124). New York: Springer Science+Business Media.

Newmark, N. M., & Rosenblueth, E. (1971). *Fundamentals of Earthquake Engineering.* Englewood Cliffs, USA: Prentice-Hall.

Norris, J. R. (1998). *Markov Chains.* Cambridge: Cambridge University Press.

Papageorgiou, A. S., & Constantinou, A. G. (1990). Response of sliding structures with restoring force to stochastic excitation. *Probabilistic Engineering Mechanics, 5*(1), 19-26.

Paparizos, L. G., & Iwan, W. D. (1988). Some Observations on the Random Response of an Elasto-Plastic System. *ASME Journal of Applied Mechanics, 55*(4), 911-917.

Ricker, N. (1953). The form and laws of propagation of seismic wavelets. *Geophysics, 18*(1), 10-40.

Sarkisian, M., Lee, P., Long, E., Shook, D., & Díaz, A. (2013). Experiences with Friction PendulumTM seismic isolation in California. *WIT Transactions on the Built Environment, 132*, 357-368.

Shang, J., Tan, P., Zhang, Y., Han, J., & Qin, J. (2021). Experimental and analytical investigation of variable friction pendulum isolator. *Engineering Structures, 243*, 112575.

Tajimi, H. (1960). A Statistical Method of Determining the Maximum Response of a Building Structure During an Earthquake. *Proceedings of the Second World Conference on Earthquake Engineering* (pp. 781-797). Tokyo, Japan: Science Council of Japan.

Tan, P., Shang, J., Han, J., Yang, K., & Zhang, Y. (2023). Experimental and Analytical Investigation of Variable Curvature and Friction Pendulum Isolator. Torino, Italy: Proceedings of the World Conference on Seismic Isolation 2022.

Trifunac, M. D., & Brady, A. G. (1975). A study on the duration of strong earthquake ground motion. *Bulletin of the Seismological Society of America, 65*(3), 581-626.